

Diffusion membrane potential in liposomes: setting by ion gradients, absolute calibration and monitoring of fast changes by spectral shifts of diS-C₃(3) fluorescence maximum

Jaroslav Večer^{*}, Petr Heřman, Aleš Holoubek

Department of Biophysics, Institute of Physics, Charles University, Ke Karlovu 5, 12116 Prague, Czech Republic

Received 9 September 1996; revised 4 December 1996; accepted 9 December 1996

Abstract

A novel fluorescent technique for direct assessment of membrane potential was tested on suspensions of large unilamellar vesicles (LUV). The method is based on monitoring shifts in the fluorescence maximum, λ_{\max} , of the redistribution dye diS-C₃(3) caused by dye binding to the LUV membrane. A theory describing the behavior of this dye in LUV suspensions was elaborated and tested. The diffusion potentials across the LUV membrane were adjusted by ion gradients in the absence of valinomycin. When using KCl and choline chloride without valinomycin the potential can be set as high as -70 mV. These potentials exhibited long-term stability and the theory allowed to determine the upper limits of membrane permeabilities for Cl⁻, choline cations, protons and hydroxyls relative to the K⁺ permeability. The absolute values of membrane potential set by ion gradients were calibrated using valinomycin. The monitoring of the λ_{\max} shift permitted us to show real-time changes in membrane potential, since addition of valinomycin to the LUV was followed by an immediate depolarization. The setting of the potential and the dye re-equilibration after valinomycin addition took place within a second.

Keywords: Slow dye; Carbocyanine; Membrane permeability; Large unilamellar vesicle; Ion gradient; Transient effect

1. Introduction

The fluorescent probe 3,3'-dipropylthiacarbocyanine iodide (diS-C₃(3)) is a redistribution dye recently used for the assessment of the Nernstian membrane potential in living cells [1–6]. This dye is a close relative to the well-known potential-sensitive carbocyanine dye diS-C₃(5) but it lacks the tendency to form nonfluorescent aggregates at high dye con-

centrations that was reported for diS-C₃(5) (for review see Ref. [7]). In contrast to the decrease of fluorescence intensity observed for diS-C₃(5), the use of the positively charged diS-C₃(3) results in an increase of the intensity upon the dye accumulation inside the cell. DiS-C₃(3) is known to redistribute between an extracellular medium and a cell interior according to the Nernst equation [8]. After penetration into the cell, a fraction of diS-C₃(3) binds to cellular structures (e.g., lipids, proteins, membranes, nucleic acids, etc.) [4,9].

In suspensions one cannot easily distinguish be-

^{*} Corresponding author. Fax: +42 2 296764. E-mail: Vecer@karlov.mff.cuni.cz

tween fluorescence originating from the extra- and intracellular medium, respectively. Fortunately, the bound form of the dye exhibits different spectral and fluorescence decay characteristics in comparison with the free dye [3,4,6,10]. This difference makes it possible to track changes of both intra- and extracellular free dye concentrations which are essential for evaluation of diffusion membrane potential.

Liposomes are much simpler objects compared to cells. Large unilamellar vesicles (LUV) are well-defined objects with no active ionic transport and with a membrane lacking proteins. The lipid bilayer is the only structure to which the dye can bind to change its spectral characteristics.

Charged redistribution dyes are known to suffer from their strong adsorption to surfaces of cuvettes, stirrers, test tubes, etc. This leads to time-dependent changes of dye concentration in solutions. This drawback often hampers the reproducibility of experiments based on simple intensity measurements. We therefore tried to establish a procedure that would be less sensitive to this effect. The adsorption of the dye changes the total fluorescence intensity but there is essentially no change in the position of the overall fluorescence maximum. Measuring the position of the fluorescence maximum, λ_{max} , therefore gives sufficient information for assessment of membrane potential.

2. Materials and methods

The fluorescent dye diS-C₃(3) was purchased from Molecular Probes (Eugene, OR), egg-yolk lecithin and TRIZMA-BASE from Sigma (St. Louis, MO), valinomycin and all other reagents (all of analytical grade) were obtained from Fluka (Buchs, Switzerland).

Tris buffer was made by titrating 50 mM TRIZMA-BASE solution in distilled water to pH 7.5 by HCl; TK, TCh, and TNa buffers were made from the Tris buffer by an addition of KCl, choline chloride, and NaCl, respectively, to reach the final concentration of 150 mM.

2.1. Preparation of liposomes

Lipid dissolved in chloroform was dried under nitrogen and kept in a high vacuum for at least 15

min. The lipidic film formed on a test tube wall was then hydrated in TK buffer and hand-shaken multilamellar vesicles (MLV) were formed. The final concentration of the lipid in the suspension was 20 mg/ml. Large unilamellar vesicles were extruded through a polycarbonate filter with a pore size of 400 nm using the LiposoFast extrusion apparatus from Avestin (Ottawa, Canada) manufactured according to the paper by MacDonald et al. [11].

2.2. Adjustment of membrane potential and labelling

The suspension of LUVs was first prediluted by TK buffer, final dilution being done by TCh buffer to obtain the required K⁺ gradient on the LUV membrane and the final lipid concentration of 1.7 mg/l, unless otherwise stated. Osmotic effects due to the difference in extra- and intraliposomal KCl concentrations were compensated by choline chloride or sodium chloride. The value of transmembrane diffusion potential $\Delta\phi$ in the presence of 10 nM K⁺-selective ionophore valinomycin was calculated from the Nernst equation. Using this procedure we were able to adjust the diffusion membrane potential in the range from 0 mV to approx. –150 mV (negative inside).

The suspension of LUV was labeled by adding the stock solution of 1×10^{-3} M diS-C₃(3) in ethanol to reach a final concentration of 2×10^{-7} M in every sample.

2.3. Fluorescence measurements

An apparatus for steady-state fluorescence experiments comprised an Ar⁺ laser excitation source (Spectra Physics, Model 171, Mountain View, CA) operating in a CW light stabilization mode at 514.5 nm and an optical multichannel analyzer OMA2 (EG & G PARC, Princeton, NJ) equipped with a SIT detector (512 channels). In order to suppress stray light, fluorescence was collected through a long-pass filter (No. 1752, Zeiss-Jena, Jena, Germany) positioned in front of the input slit of the polychromator (HR 320, Instruments SA, Inc., Metuchen, NJ). Samples in glass cuvettes were placed in a thermostated holder and gently mixed by a glass-covered magnetic

stirrer. To avoid photobleaching the excitation beam was blocked by an electronic shutter (UniBlitz, A.W. Vincent Associates Inc., Rochester, NY) whenever fluorescence was not measured.

When rapid evolutions of fluorescence spectra were measured, the liposomes were mixed with valinomycin in a special stopped-flow-like mixing device inserted in the place of the ordinary cuvette holder. Mixing of a 2-ml of sample was finished in less than one second.

3. Results and discussion

3.1. Theory of the dye response

Potential-sensitive fluorescent dye redistributes between the inner and outer spaces of liposomes according to the Nernst equation, and its free fraction in both compartments is simultaneously in an equilibrium with a fraction bound to both membrane surfaces. Because diS-C₃(3) is preferentially dissolved in an aqueous phase and exhibits very low quantum yield in a hydrophobic environment, dye molecules located inside the membrane do not contribute to the overall fluorescence intensity [8]. An equilibrium between the free (unbound) and bound dye forms can be described as:

$$K^{(m)} = [L_f]_o [D_f]_o / [D_b]_o = [L_f]_i [D_f]_i / [D_b]_i \quad (1)$$

where $K^{(m)}$ denotes an apparent dissociation constant for binding of the dye D (subscripts f and b stand for free and bound dye, respectively) to the binding sites L on the inner (i) and outer (o) membrane (m) surfaces. The concentrations $[L_f]$ and $[D_b]$ are expressed in units of surface and volume concentrations, respectively. We can assume the overall inner and outer surfaces of liposomes to be equal ($S_i = S_o = S$), with the same concentration of binding sites c_m :

$$[L_f]_o + [D_b]_o = c_m = [L_f]_i + [D_b]_i \quad (2)$$

The total fluorescence spectrum of diS-C₃(3) in the LUV suspension is a composition of the emission spectra of both free and bound forms of the dye, e.g.,

I_f and I_b , respectively. Their intensity ratio can be expressed as:

$$\begin{aligned} \frac{I_b}{I_f} &= \frac{\epsilon_b q_b (S [D_b]_o + S [D_b]_i)}{\epsilon_f q_f (V_o [D_f]_o + V_i [D_f]_i)} \\ &= \frac{\epsilon_b q_b}{\epsilon_f q_f} \frac{S}{V_o} \frac{[D_b]_o}{[D_f]_o} \frac{1 + [D_b]_i / [D_b]_o}{1 + (V_i / V_o) ([D_f]_i / [D_f]_o)} \end{aligned} \quad (3)$$

where ϵ is the extinction coefficient, q the quantum yield, V_i the intraliposomal, and V_o the extraliposomal volumes. The total volume of the suspension can be calculated as $V = V_m + V_i + V_o$, where the volume of the membrane phase V_m is much smaller than the intraliposomal volume (about 5% for our liposomes). Usually it also holds true that $V_i \ll V_o$, which simplifies Eq. (3):

$$\frac{I_b}{I_f} = K_0 \cdot \frac{[D_b]_o}{[D_f]_o} \left(1 + \frac{[D_b]_i}{[D_b]_o} \right) \quad (4)$$

where $K_0 = \epsilon_b q_b S / \epsilon_f q_f V_o$. Using Eq. (1) and Eq. (2), we can rewrite Eq. (4) as:

$$\frac{I_b}{I_f} = K_1 \left[\left(1 - \frac{[D_b]_o}{c_m} \right) + \left(1 - \frac{[D_b]_i}{c_m} \right) \frac{[D_f]_i}{[D_f]_o} \right] \quad (5)$$

where $K_1 = K_0 c_m / K^{(m)}$. When the concentration of the cationic dye in the LUV suspension is low compared with the $K^{(m)}$ value and a negative potential is present on liposomal membranes, then $[D_b]_o \ll c_m$ and Eq. (5) is reduced to:

$$\frac{I_b}{I_f} = K_1 \left[1 + \left(1 - \frac{[D_b]_i}{c_m} \right) \frac{[D_f]_i}{[D_f]_o} \right] \quad (6)$$

At very low dye concentrations one can assume that the occupation of binding sites on the inner leaflet of the membrane is also sufficiently far from saturation, e.g. $[D_b]_i \ll c_m$. Then Eq. (5) reduces even more:

$$\frac{I_b}{I_f} = K_1 \left(1 + \frac{[D_f]_i}{[D_f]_o} \right) \quad (7)$$

To use the above derived expressions for data analysis, we have to decompose the overall fluores-

cence spectrum into components corresponding to the free and bound dye forms. In time-resolved experiments one can utilize a difference in fluorescence lifetimes, in spectral measurements it is a red shift of the bound component spectrum which can be used for the decomposition. The known spectra of the free and bound dye forms were previously employed to fit the fluorescence spectrum reflecting a particular membrane potential [3]. However, it is often a time-consuming process. A procedure where the I_b/I_f is directly determined from the λ_{\max} seems to be an easier and faster approach. The dependence of λ_{\max} on I_b/I_f is then constructed only once and, using this dependence, one can find the desired intensity ratio for any λ_{\max} . Because the concentration ratio $[D_f]_i/[D_f]_o$ is unambiguously related to the diffusion membrane potential by the Nernst equation:

$$[D_f]_i/[D_f]_o = e^{-\frac{\Delta\varphi \cdot F}{RT}} \quad (8)$$

membrane potential can be directly obtained from the absolutely calibrated function $\Delta\varphi(\lambda_{\max})$. Which particular approximation has to be selected from Eqs. (5)–(7) to fit experimental data depends only on detailed experimental conditions.

When the suspension of liposomes is prepared in a solution of KCl and then diluted by a solution of choline chloride, the potential generated on the liposomal membrane can be calculated from the Goldman-Hodgkin-Katz equation which relates $\Delta\varphi$ to the transmembrane gradient of ion concentrations and to the membrane permeabilities for individual ion species:

$$\Delta\varphi = -\frac{RT}{F} \ln \left(\frac{p_K [K^+]_i + p_{Cl} [Cl^-]_o}{p_K [K^+]_o + p_{Ch} [Ch^+]_o + p_{Cl} [Cl^-]_i} \right) \quad (9)$$

$[Ch^+]$, which denotes the molar concentration of choline cations, is zero inside the LUVs at the time of dilution. If the ionic strength of the extraliposomal medium is kept constant and the suspension is n -times diluted with respect to K^+ ions, we can write for the individual ion concentrations: $c_K = [K^+]_i = [Cl^-]_i =$

$[Cl^-]_o$, $[K^+]_o = [K^+]_i/n$ and $[Ch^+]_o = [K^+]_i (n-1)/n$. Eq. (9) then can be modified:

$$\Delta\varphi = -\frac{RT}{F} \ln \left(\frac{1 + \frac{p_{Cl}}{p_K}}{\frac{1}{n} + \frac{(n-1)}{n} \frac{p_{Ch}}{p_K} + \frac{p_{Cl}}{p_K}} \right) \quad (10)$$

An addition of valinomycin to LUV suspensions substantially increases the membrane permeability for K^+ ions, $p_K \gg p_{Ch}$, p_{Cl} , which results in a simplification of Eq. (10):

$$\Delta\varphi = \frac{RT}{F} \ln \frac{1}{n} \quad (11)$$

3.2. Calibration of membrane potential

The fluorescence spectrum of free diS-C₃(3) in a buffer has its maximum at approx. 570 nm, while the bound form of the dye exhibits a red shift of 12 nm with approx. 10 times higher quantum yield [8]. Generally, the measured fluorescence spectrum, which is a composition of these two emission spectra, shifts its maximum in a spectral interval of 570–582 nm in dependence on the diffusion potential applied on the liposomal membrane. The red shift reflects the accumulation of free dye inside the liposomes and consequently an increase in the dye binding. Such dependence measured on liposomes from egg-yolk lecithin is presented in Fig. 1. To take advantage of the full spectral range available for potentials between 0 mV and –150 mV, a concentration of 1.7 mg lipid/l was selected.

After the adjustment of the required potential every sample was incubated for 1 min with diS-C₃(3) under constant stirring and the fluorescence spectrum was measured by OMA 2 (the measurement was completed within 5 s). Then valinomycin was added to a final concentration of 10 nM and an emission spectrum was immediately recorded. Finally, the position of the fluorescence maximum was extracted from a smoothed first derivative of the spectrum. Open circles in Fig. 1 represent calibration points obtained in the presence of valinomycin, closed circles refer to transmembrane potential before valinomycin was added to the suspension. Any potential obtained by the choline chloride dilution can be

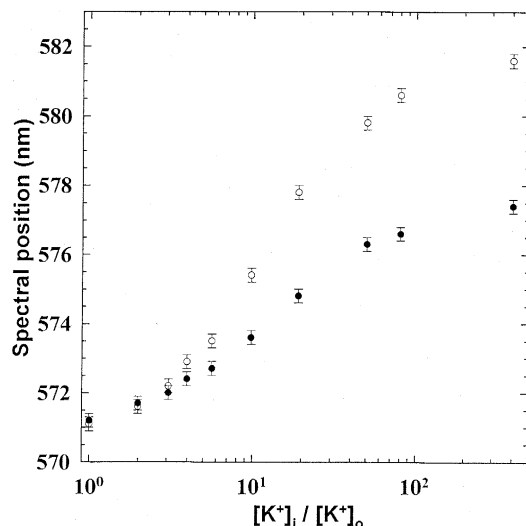


Fig. 1. Position of the fluorescence maximum of diS-C₃(3) in a liposomal suspension as a function of a potassium gradient; (○) liposomes in the presence of 10 nM valinomycin, (●) liposomes without valinomycin. The LUVs were prepared in TK buffer and diluted by TCh buffer in a proper volume ratio to obtain the required potential and a final lipid concentration of 1.7 mg/l. Concentration of diS-C₃(3) was 200 nM.

directly determined without any further assumptions from the calibration curve drawn through the calibration points. One simply takes a position of the fluorescence spectrum, finds a corresponding ratio $[K^+]_i/[K^+]_o$ from the valinomycin calibration curve, and calculates diffusion potential from the Nernst equation (Eq. (8)). Unfortunately, the analytical form of the calibration curve is unknown. The simplest way how to get the curve is to connect adjacent calibration points by a straight line; however, such a curve could be heavily influenced by experimental uncertainties. Better precision can be obtained by a model-dependent fit of the data. While a model for a direct fit of λ_{\max} vs potential is not available, the theory presented above provides ground for fitting of intensity ratios from Fig. 3A.

We have noticed (data not shown) that the fluorescence intensity of diS-C₃(3) steadily decreases with time even in a buffer mainly due to a dye trapping on cuvette walls and on the stirrer. To test this effect we measured fluorescence of 200 nM diS-C₃(3) in the TK buffer. We found a decrease in the fluorescence intensity of about 20% in 10 min (1 min overall light exposure) when the solution was placed in a glass

cuvette with a glass-coated magnetic stirrer. If a plastic stirrer was used instead of glass, up to 90% of the dye was trapped on the stirrer and cuvette surfaces in the same time period. These effects influenced the total fluorescence intensity but not the position of the fluorescence maximum in our experiments.

The λ_{\max} does not depend only on membrane potential and lipid concentration, but also on the ionic strength of the solution. There was more dye bound to the membrane if the ionic strength was lowered by changing potassium chloride concentration from 150 mM to 0 mM at $\Delta\varphi = 0$ mV. However, we did not see any spectral difference if KCl was substituted by NaCl or choline chloride of the same concentration. Therefore we kept the ionic strength constant for all our samples (see Section 2). We assume that the positively charged ions compete with the dye molecules and reduce the number of free binding sites available for the dye.

At any particular potential the λ_{\max} contains full information about the intensity ratio, and consequently about the ratio of concentrations of both free and bound forms of the dye. An alternative procedure to the spectral decomposition [3] can be employed to obtain the desired intensity ratio, as illustrated in Fig. 2: Spectra of free (in a buffer) and bound dye (at high

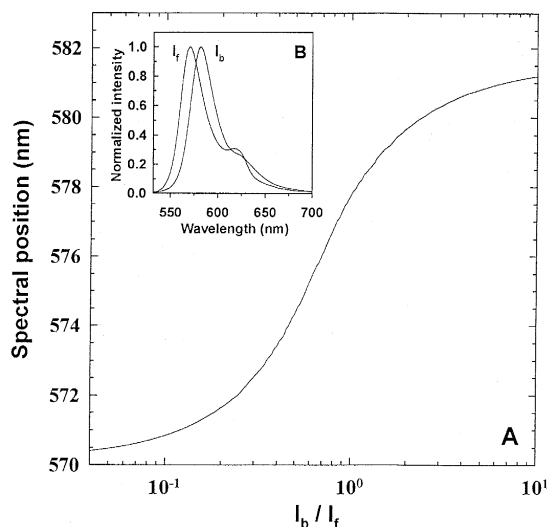


Fig. 2. Position of the fluorescence maximum as a function of the spectral ratio of the free and bound dye (A). The inset (B) shows experimentally obtained peak-height normalized spectra of free (I_f) and bound (I_b) diS-C₃(3). The spectra I_f and I_b were used to calculate the curve (A).

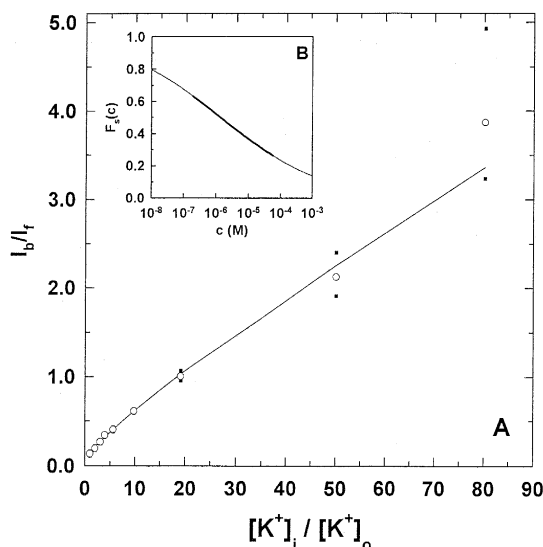


Fig. 3. Intensity ratio I_b/I_f as a function of $[K^+]_i/[K^+]_o$ (A); (○) experimental points for liposomal suspension in the presence of 10 nM valinomycin, (the I_b/I_f was obtained from the curve in Fig. 2A), (■) confidence intervals given by the precision of determination of the fluorescence maxima (± 0.2 nm), (solid line) the best fit of data by Eq. (12). For lower values of $[K^+]_i/[K^+]_o$ the confidence intervals are smaller than the size of the symbols. Inset (B) demonstrates the $F_s(c)$ as a function of the free dye concentration. The curve was calculated from the parameters of the best fit. The thick line marks a region where concentration of free dye varies in our experiment.

LUV concentration and large negative transmembrane potential) were measured and peak-height normalized (Fig. 2B). Then their composition was calculated for the intensity ratios at the respective spectral maxima ranging from 10^{-3} to 10^3 . Spectral positions of the fluorescence maxima for such calculated spectra create a sigmoidal curve shown in Fig. 2A. The curve gives an unambiguous relation between the position of the spectral maximum and the intensity ratio I_b/I_f . Now the question is how the I_b/I_f depends on the $[D_f]_i/[D_f]_o$ which is directly related to diffusion membrane potential.

The dependence of I_b/I_f on the potassium gradient $[K^+]_i/[K^+]_o$, given by the calibration curve from Fig. 1, is shown in Fig. 3A. Generally, we can take any smooth curve to fit the experimental dependence I_b/I_f vs $[K^+]_i/[K^+]_o$ without attempts at interpretation. The interpretation based on using Eqs. (5)–(7) requires two assumptions to be fulfilled: (i) The potential set by the K^+ gradient in the presence of

valinomycin is given by Eq. (11); (ii) The dye obeys Eq. (8), so we can write: $[D_f]_i/[D_f]_o = [K^+]_i/[K^+]_o$.

When using a very low dye concentration (200 nM), we can expect a linear dependence of the I_b/I_f on the free dye concentration ratio $[D_b]/[D_f]$, as described by Eq. (7). At first look a linear fit seems to be acceptable but its chi-square is too high and results of such a fit are in contradiction with Eq. (7), e.g., it is impossible to keep $K_1 = a = b$ ($I_b/I_f = a + b[K^+]_i/[K^+]_o$) as Eq. (7) requires. A likely explanation could be that even at a very low dye concentration a partial saturation of binding sites on the inner membrane side occurs.

The data from Fig. 3A can be fitted by Eq. (6) for a saturation described by $F_s(c) = 1/(1 + (Ac)^\alpha)$, where $c = [D_f]_i$ and $F_s(c)$ is a fraction of free binding sites, see e.g., [12]. However, at zero membrane potential this approximation does not give the same contribution of bound dye fluorescence from both sides of the membrane. This means that a saturation takes place even on the outer side of the membrane and Eq. (5) has to be employed for the data analysis.

The saturation of binding sites on both membrane sites should be described by the same function $F_s(c)$ which for any potential depends on corresponding free dye concentrations estimated from the intensity ratio I_b/I_f . The overall free dye concentration c_f is calculated as $c_f = (V_o/V)[D_f]_o + (V_i/V)[D_f]_i \approx [D_f]_o$, because $V_i/V \approx 10^{-6}$. The overall bound dye concentration is $c_b = (I_b/I_f)(q_f \epsilon_f / q_b \epsilon_b) c_f = (r/K_{q\epsilon})[D_f]_o$, where $r = I_b/I_f$ and $K_{q\epsilon} = q_b \epsilon_b / q_f \epsilon_f \approx 10$. The value of $K_{q\epsilon}$ is a rough estimate obtained from our measurements of fluorescence intensity and lifetimes of bound diS-C₃(3) [8]. As $c_f + c_b = c_o$ ($c_o = 200$ nM is the initial dye concentration), $[D_f]_o = c_o / (1 + r/K_{q\epsilon})$ and finally $[D_f]_i = ([K^+]_i/[K^+]_o)[D_f]_o$. Eq. (5) then gives:

$$\frac{I_b}{I_f} = K_1 \left(\frac{1}{1 + (A[D_f]_o)^\alpha} + \frac{1}{1 + (A[D_f]_i)^\alpha} \frac{[D_f]_i}{[D_f]_o} \right) \quad (12)$$

Substituting for the dye concentrations the expressions derived above, data from Fig. 3A can be fitted (solid line) giving three parameters $K_1 = 0.12$, $A = 7.3 \times 10^5 \text{ M}^{-1}$ and $\alpha = 0.28$. It should be stressed that the data has to be fitted with a correct weighing

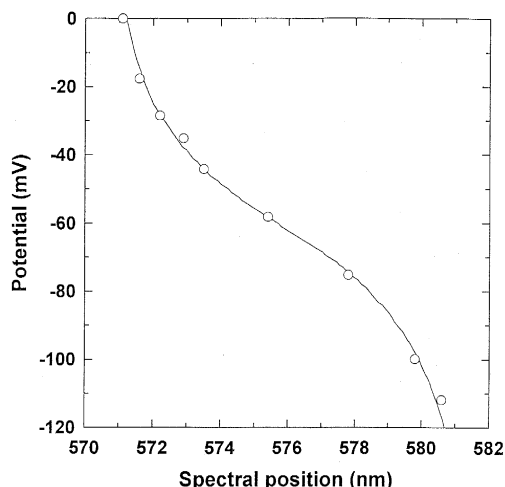


Fig. 4. Diffusion membrane potential as a function of position of the fluorescence maximum of diS-C₃(3) in the LUV suspension; (○) experimental calibration points from Fig. 1, e.g., the LUVs in the presence of 10 nM valinomycin prepared in TK buffer and diluted by the TCh buffer in a proper volume ratio to obtain the required potential, a final lipid concentration of 1.7 mg/l, and diS-C₃(3) concentration of 200 nM; (solid line) calculated calibration curve.

function accounting for standard deviations of the experimental points. Function $F_s(c)$ is shown in Fig. 3B.

Now the calibration curve can be constructed by the following procedure: The smooth curve from Fig. 2A relates any fluorescence maximum λ_{\max} to the intensity ratio I_b/I_f , the curve from Fig. 3A relates the I_b/I_f to the free dye concentration ratio $[D_f]_i/[D_f]_o$ and the transmembrane potential is calculated from Eq. (8). The final calibration curve is presented in Fig. 4 together with the experimental calibration points from Fig. 1 which were used for its calculation.

3.3. Membrane potential without ionophores

The potential generated by ion gradients without valinomycin depends on relative permeabilities of the individual ions in suspension according to Eq. (10). Values of potential extracted from our experimental data using the calibration curve from Fig. 4 are displayed in Fig. 5 (closed circles). It is seen that without valinomycin one obtains only -70 mV instead of the maximum potential of -150 mV. This is more than the value of -30 mV reported for soya

PC LUVs [13] where the potential was generated by an exchange of K^+ by Na^+ ions in the extraliposomal medium. This indicates a difference in membrane permeabilities for Na^+ and choline cations.

To estimate relative permeabilities p_{Cl}/p_K and p_{Ch}/p_K , the experimental points (Fig. 5, closed circles) were fitted by Eq. (10). Our calculations showed that the fit is not sensitive enough to find both p_{Cl}/p_K and p_{Ch}/p_K but only their sum which is smaller than about 0.07. For $p_{Cl} = 0$ m/s the best fit (Fig. 5, dashed curve) gives $p_{Ch}/p_K = 0.064$, for $p_{Ch} = 0$ m/s one obtains $p_{Cl}/p_K = 0.067$. We modeled the behaviour of $\Delta\varphi$ described by Eq. (10) for different relative permeabilities of choline and chloride ions ranging from 0. to 0.1 (Fig. 5, solid lines $p_{Ch} = 0$ m/s, dotted lines $p_{Cl} = 0$ m/s). If both permeabilities differ from zero the curve lies between the borders defined by corresponding dotted and solid lines.

To complete the discussion about the possible influence of different ions, a role of H^+/OH^- ions has to be discussed. The concentration of $[H^+]$ and $[OH^-]$ for pH 7.5 is 3.2×10^{-8} M and 3.2×10^{-7}

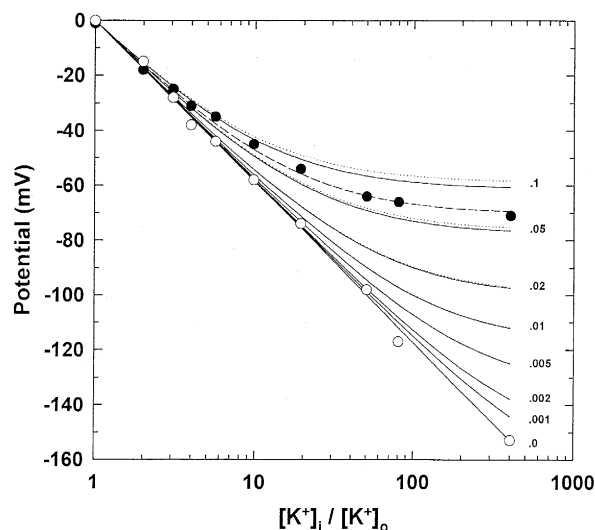


Fig. 5. Dependence of diffusion membrane potential on the $[K^+]_i/[K^+]_o$ ratio; (○) experimental calibration points: a suspension of LUV (1.7 mg/l) in the presence of 10 nM valinomycin; (●) potential values set by ions before an addition of valinomycin; (dotted line): simulated curves for $p_{Cl} = 0$ m/s, p_{Ch}/p_K changes from 0. to 0.1; (solid line): $p_{Ch} = 0$ m/s, p_{Cl}/p_K changes from 0. to 0.1; (dashed line): the best fit according to Eq. (10).

M, respectively. Assuming all permeabilities except p_K and p_H or p_K and p_{OH} to be zero, appropriately modified Eq. (10) yields the upper limit for relative permeabilities of the LUV membrane for protons and hydroxyls, e.g., $p_H/p_K < 3 \times 10^5$ and $p_{OH}/p_K < 3 \times 10^4$. For $p_K = 6 \times 10^{-13}$ m/s measured on egg-PC liposomes [14], the published proton-hydroxyl permeabilities relative to potassium permeability vary from 50 [15] to 2×10^6 [16] and the values are sensitive to a number of factors, e.g., pH or weak acid contaminants [17]. Our limiting values lie within this range.

From our data we cannot determine which ions predominantly reduce the diffusion potential set by potassium cations, i.e., whether it is choline cation, Cl^- or proton-hydroxyl conductance. When the membrane potential is set by dilution of LUVs by the TNa buffer without valinomycin, the potential-reducing ion is obviously sodium because the replacement of NaCl by choline chloride leads to hyperpolarization.

3.4. Stability of membrane potential

In contrast to the valinomycin method, the potentials set by ions without valinomycin are lower but

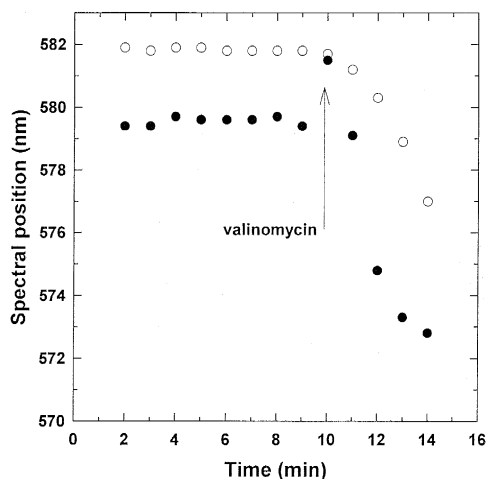


Fig. 6. Time behavior of the spectral maximum for liposomal suspension stained by diS-C₃(3). The positions of the fluorescence maxima were read from a set of 32 time-resolved fluorescence spectra measured at 60-s intervals. Liposomes (6.3 mg of lipids/l, stained with 200 nM dye) were prepared in TK buffer and then diluted by TCh (○) or TNa (●) buffers to obtain a $[K^+]_i/[K^+]_o$ ratio of 400:1. An arrow indicates the time of addition of valinomycin (its final concentration was 1 μ M).

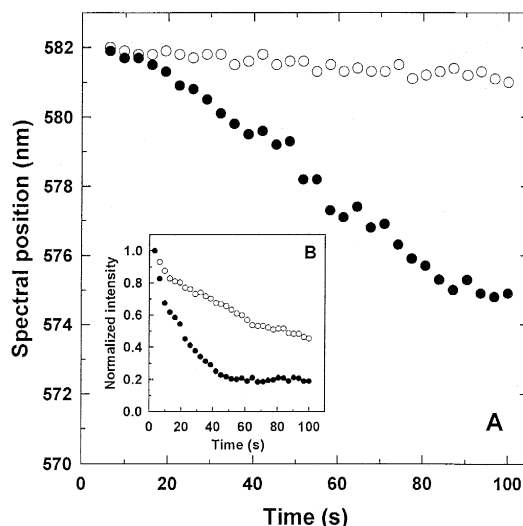


Fig. 7. Time evolution of the position of the spectral maximum (A) and fluorescence intensity (B) for liposomes stained with diS-C₃(3) after addition of valinomycin. The positions of the fluorescence maxima were read in 3-s intervals. Liposomes (6.3 mg of lipids/l, stained with 200 nM dye) were prepared in TK buffer and then diluted by TCh (○) or TNa (●) buffers to obtain a $[K^+]_i/[K^+]_o$ ratio of 400:1. The final concentration of valinomycin was 1 μ M.

more stable over long periods of time. We tested this time stability. The LUVs were diluted with either TCh or TNa buffers to generate membrane potential, stained, and the fluorescence was measured after two min at 1-min intervals. Fig. 6 shows that there is no detectable change in the position of the fluorescence maximum as long as valinomycin is absent. For LUVs with the K^+/Na^+ gradient on the membrane (closed circles) an addition of valinomycin ($c = 1$ μ M) causes hyperpolarization which is reflected by a red shift of the fluorescence spectrum (open circles). No spectral shift can be detected for the LUVs with the $K^+/choline^+$ gradient because 582 nm is already the limiting value. As seen from Fig. 6, the hyperpolarization is followed by a fast depolarization indicated by a blue shift of the spectra for both types of liposomes. To monitor more closely the behavior of liposomal suspensions immediately after the addition of valinomycin, we measured the spectral evolution with the time resolution of seconds (Fig. 7). The valinomycin-induced hyperpolarization as well as the reequilibration of the dye through the liposomal membrane after addition of valinomycin were found

to be fast processes. However, the data also demonstrate that the potential starts to fall instantly. The observed depolarization is much faster for K^+/Na^+ liposomes than for $K^+/choline^+$ ones. This is consistent with literature reports [13,14,18], on valinomycin-induced macroscopic changes of ion concentrations. Similar behavior, but with a lower rate constant, was detected even at very low valinomycin concentrations ($c = 1$ nM, data not shown). As expected, the observed depolarization was accompanied by a simultaneous decrease in fluorescence intensity measured at a maximum of the fluorescence spectrum, Fig. 7B. We assume that the valinomycin-induced depolarization can be the result of a nonspecific increase in membrane permeability for ions different from K^+ due to perturbations of the membrane caused by transitions of relatively large valinomycin molecules through the lipid bilayer. The size of such perturbations could explain the faster depolarization rate in the presence of Na^+ compared to the rate in the presence of the larger choline cations (Fig. 7). The increased ion fluxes then result in macroscopic changes of ion concentrations and consequently in depolarization.

In experiments with a higher time resolution, two equal volumes of the sample were quickly mixed. The first one contained stained liposomes with the $[K^+]_i/[K^+]_o$ ratio of 400:1, the second one a mixture of TCh and TK buffers in the same ratio (v/v) plus valinomycin. On mixing the two components, the potential changed from -70 mV to -150 mV (Fig. 5), and dye reequilibration started because the equilibrium dye concentration ratio $[D_f]_i/[D_f]_o$ had to change from approx. 15 to 400. As the total dye concentration was two times higher before mixing, the absolute intraliposomal dye concentration $[D_f]_i$ had to increase more than 10 times after reequilibration. Nevertheless, as demonstrated in Fig. 7 and even with the time resolution of 0.5 s (data not shown), the processes of hyperpolarization and the subsequent dye reequilibration were not detected. This means that these two processes had been finished in less than one second.

3.5. Conclusions

The assessment of diffusion membrane potential from the position of the fluorescence maximum for a

two-state system such as diS-C₃(3) in LUV suspensions is a useful technique for rapid monitoring of transmembrane potential. The theory presented in this paper gives a direct relation between the position of the fluorescence maximum and the membrane potential applied on liposomes. Experimental data indicate a nonlinear relation between the intensity ratio I_b/I_f and the dye concentration ratio $[D_f]_i/[D_f]_o$. Diffusion membrane potential adjusted by ion gradients without valinomycin exhibits a long-term stability and a value as high as -70 mV can be adjusted with the aid of choline chloride. However, membrane permeabilities for all ion species present in the suspension has to be taken into account when the membrane potential is evaluated. In the presence of valinomycin the diffusion membrane potential set dominantly by a K^+ gradient follows the Nernst equation at the time of valinomycin addition but an immediate depolarization, the rate of which depended on valinomycin concentration, sets in. Upper limits for the relative membrane permeabilities of Cl^- , choline cations, protons and hydroxyls were estimated for LUVs made from egg-yolk lecithin: $p_{Cl}/p_K < 0.067$, $p_{Ch}/p_K < 0.064$, $p_H/p_K < 3 \times 10^5$, $p_{OH}/p_K < 3 \times 10^4$. Both the dye reequilibration and the valinomycin-induced change of membrane potential were shown to be finished in less than a second.

There are two main applications of the methods described above. The first, suspensions ones calibrated (e.g., as in Fig. 5) can be prepared by an identical procedure later and any stable diffusion membrane potential can be adjusted without additional calibrations. Both positive and negative potentials are available when intra- and extraliposomal ion concentrations are exchanged by each other. The second application covers real-time measurements of the membrane potential in liposomal suspensions. The transients can be measured either absolutely on calibrated suspensions (see Fig. 4 for calibration) or qualitatively only, as was demonstrated by the depolarization process following an addition of valinomycin (Figs. 6 and 7).

Acknowledgements

This work was supported by GAUK-167/96 and GAUK-168/96 grants. The authors wish to thank Dr.

J. Plášek and Dr. K. Sigler for critical reading of the manuscript and stimulating discussions.

References

- [1] Haugland, P.R. (1992–1994) *Handbook of Fluorescent Probes and Research Chemicals*, 5th edn., Molecular Probes, Eugene, OR, USA.
- [2] Peña, A., Uribe, S., Pardo, J.P. and Borbolla, M. (1984) *Arch. Biochem. Biophys.* 231, 217–225.
- [3] Plášek, J., Denksteinová, B. and Sureau, F. (1993) *J. Fluorescence* 3, 157–159.
- [4] Plášek, J., Dale, R.E., Sigler, K. and Laskay, G. (1994) *Biochim. Biophys. Acta* 1196, 181–190.
- [5] Gášková, D., Kurzweilová, H., Denksteinová, B., Heřman, P., Večeř, J., Sigler, K., Plášek, J. and Malínský, J. (1994) *Folia Microbiol.* 39, 523–525.
- [6] Denksteinová, B., Gášková, D., Heřman, P., Večeř, J., Sigler, K. and Plášek, J. (1996) in *Fluorescence Spectroscopy and Fluorescence Probes* (Slavík, J., ed.), pp. 151–156, Plenum Press, New York.
- [7] Smith, J.C. (1990) *Biochim. Biophys. Acta* 1016, 1–28.
- [8] Heřman, P., Večeř, J. and Holoubek, A. (1996) in *Fluorescence Spectroscopy and Fluorescence Probes* (Slavík, J., ed.), pp. 139–144, Plenum Press, New York.
- [9] Plášek, M. and Sigler, K. (1996) *J. Photochem. Photobiol. B* 33, 101–124.
- [10] Heřman, P., Večeř, J., Denksteinová, B., Gášková, D., Plášek, J., Kurzweilová, H., Sigler, K. and Sureau, F. (1994) *Folia Microbiol.* 39, 535–538.
- [11] MacDonald, R.C., MacDonald, R.I., Menco, B.P.M., Takeshita, K., Subbarao, N.K. and Hu, L. (1991) *Biochim. Biophys. Acta* 1061, 297–303.
- [12] Cantor, Ch.R. and Shimmel, P.R. (1980) *Biological Chemistry; The Behavior of Biological Molecules*, Vol. 3, W.H. Freeman, San Francisco.
- [13] Hope, M.J., Bally, M.B., Webb, G. and Cullis, P.R. (1985) *Biochim. Biophys. Acta* 812, 55–65.
- [14] Venema, K., Gibrat, R., Grouzis, J.P. and Grignon, C. (1993) *Biochim. Biophys. Acta* 1146, 87–96.
- [15] Gutknecht, J. and Walter, A. (1981) *Biochim. Biophys. Acta* 641, 183–188.
- [16] Nichols, J.W., Hill, M.W., Bangham, A.D. and Deamer, D.W. (1980) *Biochim. Biophys. Acta* 596, 393–403.
- [17] Gutknecht, J. (1987) *Biochim. Biophys. Acta* 898, 97–108.
- [18] Blok, C.M., De Gier, J. and Van Deenen, L.L.M. (1974) *Biochim. Biophys. Acta* 367, 202–209.